Robotics and Autonomous Systems 76 (2016) 36–45

Contents lists available at ScienceDirect

Robotics and Autonomous Systems

journal homepage: www.elsevier.com/locate/robot

Side-to-side 3D coverage path planning approach for agricultural robots to minimize skip/overlap areas between swaths

I.A. Hameed [a,*], A. la Cour-Harbo [b], O.L. Osen [a]

[a] Norwegian University of Science and Technology, Faculty of Engineering and Natural Sciences, Department of Automation Engineering, Larsgårdsvegen 2, 6009 Ålesund, Norway

[b] Aalborg University, Faculty of Engineering and Science, Department of Electronic Systems, Section of Automation and Control, Fredrik Bajers Vej 7C, 9220 Aalborg, Denmark

HIGHLIGHTS

- We developed a more efficient 3D field coverage approach compared to existing approaches.
- We developed a numerical approach to examine the efficiency of 3D coverage algorithms in terms of skip/overlap areas.
- We developed side-to-side 3D field coverage approach, which ensure 100% coverage regardless of the topographical nature of the field surface.
- Simulation and real field experiments are conducted to prove the efficiency and superiority of the developed approaches.

ARTICLE INFO

Article history:
Received 7 January 2015
Received in revised form
10 November 2015
Accepted 16 November 2015
Available online 3 December 2015

Keywords:
Area coverage planning
Coverage efficiency
Side-to-side 3D coverage planning
Robotics
Optimization

ABSTRACT

Automated path planning is an important tool for the automation and optimization of field operations. It can provide the waypoints required for guidance, navigation and control of agricultural robots and autonomous tractors throughout the execution of these field operations. Typical field operations are repetitively required nearly every cropping season and therefore it should be carried out in a manner that maximizes the yield and minimizes operational cost, time and environmental impact taking into account the topographic land features. Current 3D terrain field coverage path planning algorithms are simply 2D coverage path planning projected into 3D through field terrain represented by the field's Digital Elevation Model (DEM). When projecting 2D coverage plan into its 3D counterpart, the actual distance between adjacent paths on the topographic surface either increases or decreases, and consequently there might be skips or overlaps between adjacent paths on the slopes. In addition, when the machine rolls on slopes the effective width of the implement decreases by a similar amount to double this error and complicates the problem. Skips and overlaps can lead to an inefficient use of land and resources. In this paper, a numerical approach to estimate the total skip/overlap areas is developed and applied to determine the optimum-driving angle that minimizes this impact. Also, a novel side-to-side 3D coverage path planning approach, which ensures zero skips/overlaps regardless of the topographical nature of the field terrain, is developed. The approaches developed in this paper are tested and validated using a hypothetical test field of a tailored terrain and a real experimental field of uneven terrain nature. The proposed approaches illustrated that a significant percentage of uncovered area could be saved if appropriate driving angle is chosen and if a side-to-side 3D coverage is used.

1. Introduction

Robots, for long decades, have played a fundamental role in increasing the efficiency and reducing the cost of many industries and products. Robots are used for tasks when there are concerns over human safety, or when the task is repetitive and can be done more productively by a robot working longer hours than humans and offer a precision that humans cannot provide. The agricultural industry is no different in this regard. In the last two decades, a similar trend has started to take place in agriculture, which is suffering from shortage of skilled and unskilled labor workforce. With GPS- and vision-based self-guided tractors and harvesters already being available commercially, farmers have started to

* Corresponding author.
E-mail address: ibib@ntnu.no (I.A. Hameed).

http://dx.doi.org/10.1016/j.robot.2015.11.009
0921-8890/

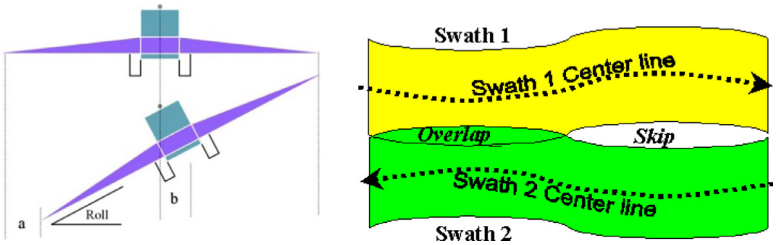

(a) Illustration of roll effect on effective width; *a* is the reduction of effective boom width while *b* is the lateral translation of implement [12].

(b) Conceptual diagram of overlap and skip areas between two adjacent swaths caused by variation of slope from pass to pass [17].

Fig. 1. Effect of roll on machine coverage.

experiment with autonomous systems that automate typical field operations such as harvesting, mowing, spraying, and weed removal [1]. Automated path planning is an important tool for automation and optimization of field operations. It is used to provide a complete trajectory for guidance, navigation and control of agricultural robots and autonomous tractors throughout the execution of these field operations [2,3].

Currently, most coverage path planning algorithms are only capable of dealing with fields on 2D terrain [4–6]. Optimization algorithms have been developed to optimally select driving angle and sequence of tracks of these 2D driving patterns so that field operations can be carried out in a manner that reduces maneuvering over the field surface and total operational time and in turn reduces soil compaction, fuel consumption and henceenvironmental impact [7–10]. 2D coverage path planning algorithms are based on the assumption that most agricultural fields are flat and hence ignore elevation changes. It has been observed that important information is lost when elevation changes are ignored which deteriorates the optimization process and thus gives inferior design of the coverage paths [11]. The terrain characteristics have significant influence on the design and optimization of the coverage path planning. A great proportion of farms have rolling terrains, which have considerable influences on the design of coverage paths, for example, 47% of cropland in the United States is no less than 2% slopes; 48% of the cropland is on slopes between 2% and 10% [12]. Koostra et al. [13] showed that the error between planimetric and topographic surface area could be as much as 5% in typical farm fields. Dilon et al. [14] demonstrated that these area discrepancies are economically significant, especially when considered over multiple field operations. Therefore, a new coverage path planning considering the terrain characteristics is expected to have a great potential to further optimize field operations.

Despite its importance in the optimization of field operations and accurate navigation of agricultural robots and autonomous tractors, 3D terrain field coverage path planning did not attract the expected attention from researchers. Only limited research on developing area coverage planning for 3D terrain has been reported. For example, Jin and Tang [15] developed an optimized 3D terrain field coverage path planning algorithm that classifies the field terrain into flat and sloppy areas and then applies the most appropriate path planning strategy to each region in terms of minimized headland turning cost, soil erosion cost, and skip/overlap area cost. Hameed et al. [8,9] developed a simple and effective approach for 3D terrain path planning where the 2D path planning was first generated and then projected through the field's DEM. Based on this approach, Hameed [16] developed an optimization algorithm which can optimize the driving angle and sequence of tracks over 3D terrain so that field operations can be carried out in a manner which reduces operational time, fuel consumption, and non-productive traveled distance and maneuvering over the field surface.

The objective of this paper is to develop an approach to estimate the total skipped/overlapped areas between field rows when projecting 2D coverage path into 3D coverage path through DEMs. This approach will be used to find the optimal driving angle that minimizes the skipped/overlapped areas and hence reduces its economical impact. In addition, a new 3D coverage approach is proposed which can provide full coverage regardless of the terrain structure of the field. The developed approaches are applied to typical (synthesized) field terrain and two real fields.

The paper is organized as follows; initially, a simple 2D coverage approach is introduced in Section 2.1. Next, a 3D terrain modeling and interpolation is presented in Section 2.2. The impact of projecting 2D planning into its 3D counterpart is then presented in Section 2.3. In Section 2.4, a complete side-to-side 3D coverage approach that ensures full coverage regardless of the terrain structure is introduced. In Section 3, a number of experiments are performed to test and validate the developed approaches. Finally, a brief concluding remarks and future work are presented in Section 4.

2. Methodology

2.1. Background

The basic assumption that most agriculture fields are flat and ignoring elevation changes across the field has lead to some problems not only with 2D path planning but also with 3D path planning obtained from projecting the resultant 2D path planning through the field terrain. When projecting 2D planning result to 3D terrain, the actual distance between paths on the topographic surface either increases or decreases, consequently, there will be skip and/or overlap areas between adjacent paths on the slopes, as it isshown in Fig. 1(a). Former researchers figured out that this area discrepancy between planimetric and topographic models is significant and might result in economic impacts, especially when considered over multiple field operations [13,14]. Topography can have an impact on machine travel patterns in the field, which in turn will affect the application coverage [12]. This impact becomes evident if the machine is utilizing some form of GPS-based guidance system, which is not considering the vertical (i.e., elevation) component of position. This will have several impacts on the effective coverage of the machine. If the machine is experiencing some roll (sideways tilt), its planimetric or effective width decreases which makes the problem even worse as it is obvious in Fig. 1(b). Similarly for a given swath spacing, the actual distance between paths on the topographic surface increases. The spacing increase is the same as the machine width decrease essentially doubling the error. The result is that there will be skips on steeper side slopes and vice versa [12]. Further complicating the effect of machine roll is the fact that the GPS antenna is mounted on the top middle of the machine. As the machine rolls, if there is

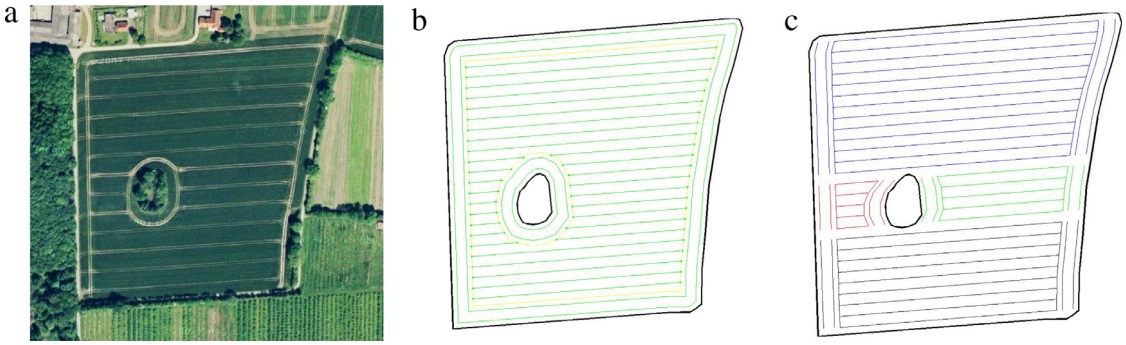

Fig. 2. An illustrative example of the 2D geometrical field representation: (a) satellite image of a field of an area of around 5.54 (ha) located in [+54° 57′8.28″ N, + 9° 46′ 49.31″E], (b) driving pattern for a driving angle of 4.5°, working width of 9 m and two headland polygons, and (c) driving pattern for two headland paths at both sides of the field tracks where field tracks are clustered into blocks [8,9].

no measurement and compensation of roll in the GPS position, the guidance system will attempt to keep the antenna on the desired path instead of the centerline of the machine. This will cause the machine implement (e.g., spray boom, planter or tillage tool) to actually translate to the side of the desired path.

This translation will not affect coverage if the roll is constant from one path to the next since translation on each pass will be the same amount in the same direction. The translation becomes critical as the slope varies from pass to pass, for example, at a translation from higher flat area to a downward slope, adjacent swaths could overlap. Likewise, a skip could be produced on a translation from a slope to a lower flat, as it is shown in Fig. 1(b). Stombaugh et al. [12] pointed out that manufactures of guidance and automated steering systems are attempting to compensate for translational effect caused by topography by incorporating roll measurement and compensation devices into their equipment. However, the problem remains as long as the resultant path is obtained through simple projection through DEMs without incorporating the topographical effect in the coverage path design. Therefore, the objective here is to incorporate the topographical effect of the field terrain in the design of the 3D coverage path to minimize the skips between adjacent swaths. Two algorithms are proposed. First, an algorithm to numerically evaluate the total skips in current conventional 3D coverage algorithms, which is based on projection through field terrain and provides farmers with the optimum driving angle that minimizes the total skips and/or overlaps. Second, an enhanced 3D side-to-side coverage algorithm is proposed in which spaces between adjacent swaths are kept equal taking into account the topographical nature of the field.

2.2. 2D coverage path planning

Field coverage is the process in which a driving pattern is generated to guide an autonomous tractor or a robot to cover a crop field in a systematic way and in a manner which reduces operational time, maneuvering over the field surface, soil compaction, fuel consumption, etc. These patterns can be represented by a set of waypoints representing field tracks and headland polygons parallel to a predefined driving direction and within a certain operating width between its swaths. In recent years, many field coverage approaches have been developed [18,4–6,19,7].

The inputs to such methods are; (1) the field outer boundaries as a set of coordinates, (2) driving angle (basically the driving direction as a compass direction in degrees), and (3) the number of headland paths (i.e., chosen based on the operating width and minimum turning radius of the vehicle). The outputs are; (1) a set of waypoints representing field tracks, and (2) a set of waypoints representing headland paths or polygons (as it is shown in Fig. 2). Headland paths could be in the form of closed polygons adjacent to field outer boundaries and permanent obstacles, as it is shown in Fig. 2(b), and this type requires more computational time to provide more smoothed polygons. Alternatively, headland paths could be generated at both sides of the field tracks, as it is shown in Fig. 2(c) and this approach provides headland paths similar to what human drivers used to do when they drive in the field and this approach is three times faster than generating headland paths as closed polygons because it does not require smoothing which is computationally exhaustive [8,9].

2.3. Rapid 2D/3D path planning

In 2D coverage path planning approaches, each field track/swath is defined by two waypoints, namely, starting and ending waypoints. To map the 2D coverage path into its 3D counterpart, the track line is sampled to generate intermediate waypoints at distance less than the grid cell size. These points are then mapped through the field terrain to find the elevation of each intermediate point. Terrain's surfaces are represented in 3D using digital elevation model (DEM), which is a grid of squares representing elevations. DEMs are commonly built using data collected using remote sensing techniques, but they may also be built from land surveying. This process is carried out track-by-track and hence time consuming and not practical for optimization algorithms such as Genetic algorithms (GAs) and does not ensure full coverage [8,9].

In this paper, a new 2D/3D field coverage approach is developed, in which field tracks are generated and mapped directly. In this approach, the minimum bounding box (MBB), which is the smallest enclosing box of the set of points representing the field's boundaries, is first determined. MBB is then extended by a distance (e.g., half the circumradius of the field's outer polygon or the field's MBB) to ensure full coverage when the grid is rotated to match the required driving angle. The EMBB is then divided along its X- and Y-axes into cells, so that each cell within the grid is a rectangle of length l and width w in meters. Cell length, l, is used to define the precision of the resultant 3D tracks while cell width, w, is used to define the operating width of the vehicle or implement or the effective distance between swaths, as it is shown in Fig. 3(a). Cell length, l, is usually chosen as a trade-off between resolution and computational complexity. Fig. 3(b) shows the coordinate grid of an EMBB of a real field for a driving angle $\theta = 90°$, $l = 0.1$ m, $w = 10$ m. Driving angle is defined as the angle between the horizontal axis, X-axis, and the required driving direction. The vertical grid lines (blue lines) shown in Fig. 3(b) which are represented as a set of points at distance, l, are considered as potential field tracks.

Once the coordinated grid is obtained, the grid can then be rotated by an angle, θ, counter clockwise around its center point,

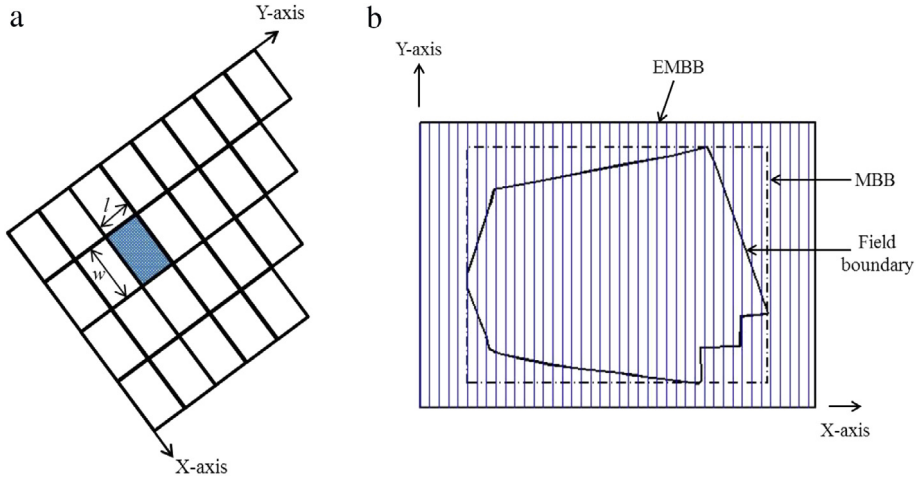

Fig. 3. Grid based 2D/3D coverage approach. (For interpretation of the references to colour in this figure legend, the reader is referred to the web version of this article.)

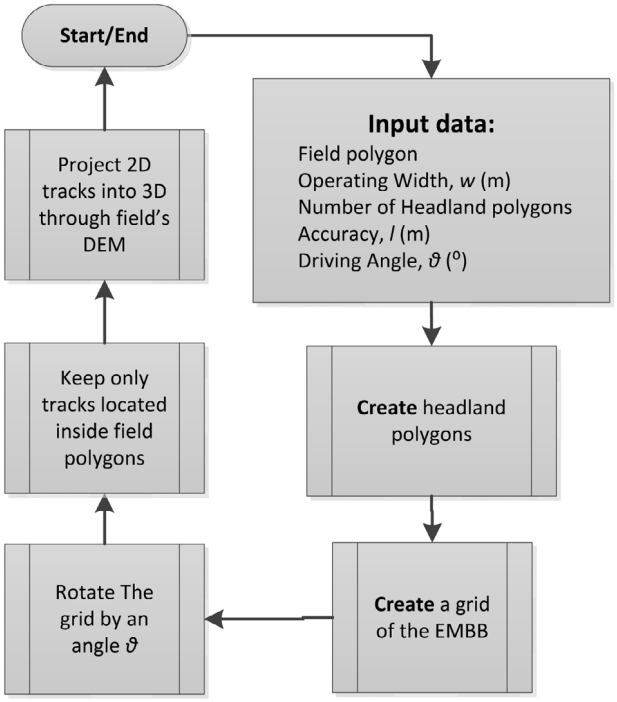

Fig. 4. Flowchart of the developed 2D/3D field coverage approach.

(x_c, y_c), using Eq. (1) where each primitive or point (x, y) is first rotated by an angle θ around the origin and then translated in the direction of the center point, (x_c, y_c) to then translated back again to its original location.

$$\begin{bmatrix} x' \\ y' \\ 1 \end{bmatrix} = \begin{bmatrix} \cos(\theta) & -\sin(\theta) & x_c \\ \sin(\theta) & \cos(\theta) & y_c \\ 0 & 0 & 1 \end{bmatrix} \cdot \begin{bmatrix} x \\ y \\ 1 \end{bmatrix},$$

$$\begin{bmatrix} x_\theta \\ y_\theta \\ 1 \end{bmatrix} = \begin{bmatrix} \cos(\theta) & \sin(\theta) & -x_c\cos(\theta) - y_c\sin(\theta) \\ -\sin(\theta) & \cos(\theta) & x_c\sin(\theta) - y_c\cos(\theta) \\ 0 & 0 & 1 \end{bmatrix} \cdot \begin{bmatrix} x' \\ y' \\ 1 \end{bmatrix}. \quad (1)$$

The final 3D tracks can then be obtained through filtering where points, which are not located inside the field polygon, are discarded (this can easily done using a Matlab™ function called *inpolygon* [20]). The 3D tracks are then obtained by simple projection through the DEM of the field to find elevation of each point. The approach is described by the flowchart shown in Fig. 4.

2.4. 3D terrain interpolation

Terrain representation plays a central role in environmental modeling and landscape visualization. The Digital Elevation Models (DEMs) contain elevation of discrete points measured at regular spaced intervals to represent the surface. DEMs of agricultural field terrains have an accuracy of 1.6 m. The accuracy of DEMs data has direct implications on the associated operations such as field coverage [21,22]. Before projecting a 2D driving pattern into its 3D counterpart, it is essential to interpolate the terrain in order to find elevation of positions which do not exist in DEM data. Interpolation is the first step toward accurate 3D coverage path planning. Interpolating methods were applied to estimate the elevation of any point based on the data pointsin DEMs [23].

In this paper, Bilinear Interpolation (BLI) approach is used. BI is a resampling method that uses the distance-weighted average of the four values of a grid cell to estimate a new value. Interpolation can be used to estimate the elevation of an unknown point in the terrain surface that does not exist in the DEM grid data using four input grid known neighboring points. The key idea behind BI is to: (1) perform linear interpolation along each line of latitude in the West–East direction; (2) normalize the two partial weights for each point; and finally (3) perform a linear interpolation along each line of longitude in the perpendicular (i.e., the South–North) direction, as it is shown in Fig. 5. Although each step is linear in the sampled values and in the position, the interpolation as a whole is not linear but rather quadratic in the sample location. Suppose that we want to find the value of the unknown function f at the point $P = (x, y)$ where f is the elevation at point P, x and y are the latitude and longitude of the position on the surface. It is assumed that we know the values of f at the four grid points; $f(Q_{11})$ is the elevation at $Q_{11} = (x_1, y_1)$, $f(Q_{12})$ is the elevation at $Q_{12} = (x_1, y_2)$, $f(Q_{21})$ is the elevation at $Q_{21} = (x_2, y_1)$, and $f(Q_{22})$ is the elevation at $Q_{22} = (x_2, y_2)$. We first do linear interpolation in the x-direction (i.e., West–East direction). This yield:

$$\begin{aligned} f(R_1) &\approx \frac{x_2 - x}{x_2 - x_1} f(Q_{11}) + \frac{x - x_1}{x_2 - x_1} f(Q_{21}), \\ f(R_2) &\approx \frac{x_2 - x}{x_2 - x_1} f(Q_{12}) + \frac{x - x_1}{x_2 - x_1} f(Q_{22}) \end{aligned} \quad (2)$$

where $R_1 = (x, y_1)$ and $R_2 = (x, y_2)$.

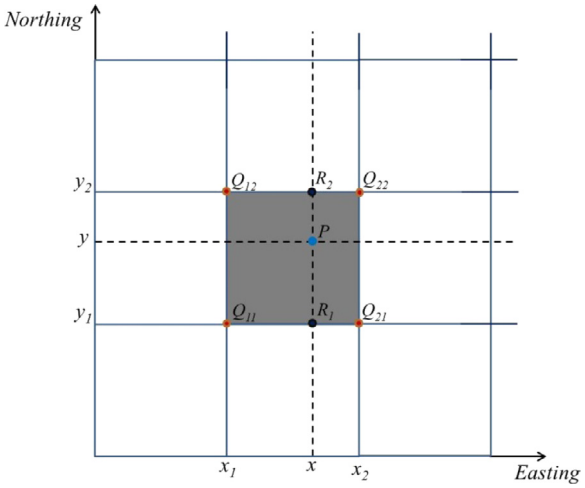

Fig. 5. The four red dots; Q_{11}, Q_{12}, Q_{21} and Q_{22} show the available four data points of a cell and the blue dot, P, is the point at which we want to interpolate to find elevation. (For interpretation of the references to colour in this figure legend, the reader is referred to the web version of this article.)

We then proceed by interpolating in the y-direction (i.e., the South–North direction) to give the desired estimate of $f(x, y)$, as follows:

$$f(P) \approx \frac{y_2 - y}{y_2 - y1} f(R_1) + \frac{y - y_1}{y_2 - y1} f(R_2). \tag{3}$$

Other methods for interpolating data points on a 2D regular grid such as Bicubic Interpolation (BCI) where the interpolated surface is smoother than the corresponding surfaces are obtained by BLI [24].

2.5. Efficiency estimation of conventional 3D coverage planning

Agriculture constantly strives for improved efficiencies. Agricultural application or swathing efficiency is one area of interest given the potential of new technology in precision farming. Tools and techniques are needed to assess application efficiency so in-field guidance techniques can be compared and quantified. One measure of application efficiency is the occurrence of overlap (double application) and skips (missed application) areas between adjacent swaths in application. Many techniques have been developed to evaluate the application efficiency in field applications [17]. These approaches were based on the assumption that most of agricultural fields are flat and spaces between swaths are fixed regardless of the topographical nature of the field terrain. Ignoring elevation change simplified the derivation process of 2D coverage path planning used in today agriculture. However, when simply projecting 2D coverage path into 3D through field terrain, new problems and challenges come up.

For a given swath spacing, the actual distance between paths on the topographic surface increases and there will be skips between adjacent paths on the slopes. If the machine is experiencing some roll (sideways tilt), its effective width decreases while spacing increases essentially doubling the error. Therefore, the need arises to develop a quantitative analysis to compare operational and topographic surfaces in terms of skips and/or overlaps to quantify this impact and to improve the application efficiency. Stombaugh et al. [12] presented an analytical approach to quantify total skip area; however, this method assumed that the entire field is in one common slope. The objective of this paper is to develop a numerical approach that is able to quantify the skips and/or overlaps of any 3D coverage plan for all driving angles with high accuracy. The approach can be potentially used to provide farmers with the driving angle which when followed can minimize the topographical impact on coverage efficiency. In addition, it will raise the concern for the need for a new enhanced 3D coverage path planning algorithm that is able to compensate for topographic impact on swath spaces.

Numerical approach

In this approach, 3D coverage path planning is quantified for skip (i.e., due to missed application) and/or overlap areas (i.e., due to double application). A coverage path planning consists of a number of headland paths/polygons and a number of parallel field tracks, as it is shown in Fig. 5(a), for a hypothesized testing field terrain of 200 m^2 flat area with a half cylinder of radius 10 m on its center to provide a simple terrain with varying sloping. The plan is generated for an effective operating width $w = 1$ m and the driving angle $\theta = 90°$. Each field track consists of a number of segments, each of length l chosen in a way to give sufficient accuracy when represented in 3D. To numerically measure the distance between tracks in 3D, a 3D cylinder of radius equal to the vehicle's operating width, w, is generated around each segment, as it is shown in Fig. 5(b). Then a fine grid is generated and projected into the field terrain. Finally, the total number of points which are located inside the 3D cylinder, N, is determined and divided by the total number of points located in the entire field, N_f, and used as an estimate of the coverage efficiency, given by Eq. (4).

$$\text{cov}_{ef} = \sum_{cy} N/N_f. \tag{4}$$

Covered area can then be obtained by multiplying the field surface area by the coverage efficiency. When the approach is applied to the 3D driving path of the field shown in Fig. 6(a), a huge number of tiny 3D cylinders of radius, w, are generated around each segment as it is shown in Fig. 6(c). Fig. 6(d) shows the field from 2D point of view where skips cannot be noticed. By comparing Fig. 6(c) and (d), it becomes obvious that the topographical nature of the field increased spaces between swaths and large areas are missing covering. In this example and for this driving angle around 16% of the field area is missing covering which can cause financial losses to farmers.

2.6. Side-by-side 3D coverage approach

The cylindrical approach for coverage efficiency assessment presented in Section 2.5 can be used to assess the application efficiency for all possible driving angles and provide farmers with the angle that minimizes the impact of the topographical nature of the field terrain and hence maximizes the coverage efficiency and yield. This process will definitely improve the land use, however, it might conflict with the optimization criterion such as maneuvering over the field surface, operational time, fuel consumption, and soil compaction. Therefore, the need arises for an approach that can achieve 100% coverage regardless of the topographical nature of the field terrain. Here, a new 3D coverage algorithm is proposed in which distance between adjacent swaths are kept equal regardless of the topographical nature of the field. The developed approach simply generates tracks side-by-side directly in the 3D representation of the field without gaps between neighboring tracks. This technique overcomes skip areas between field tracks when projecting 2D coverage plan into its 3D counterpart.

The process starts by generating a starting curve (i.e., seed curve) in the middle of the field. Once a seed curve is found, it can be offset sideways on the topographic surface of the field for generating the subsequent paths, and this process continues until the whole field surface is fully covered. A 3D cylinder is generated around the seed curve. Two neighboring tracks are obtained as the

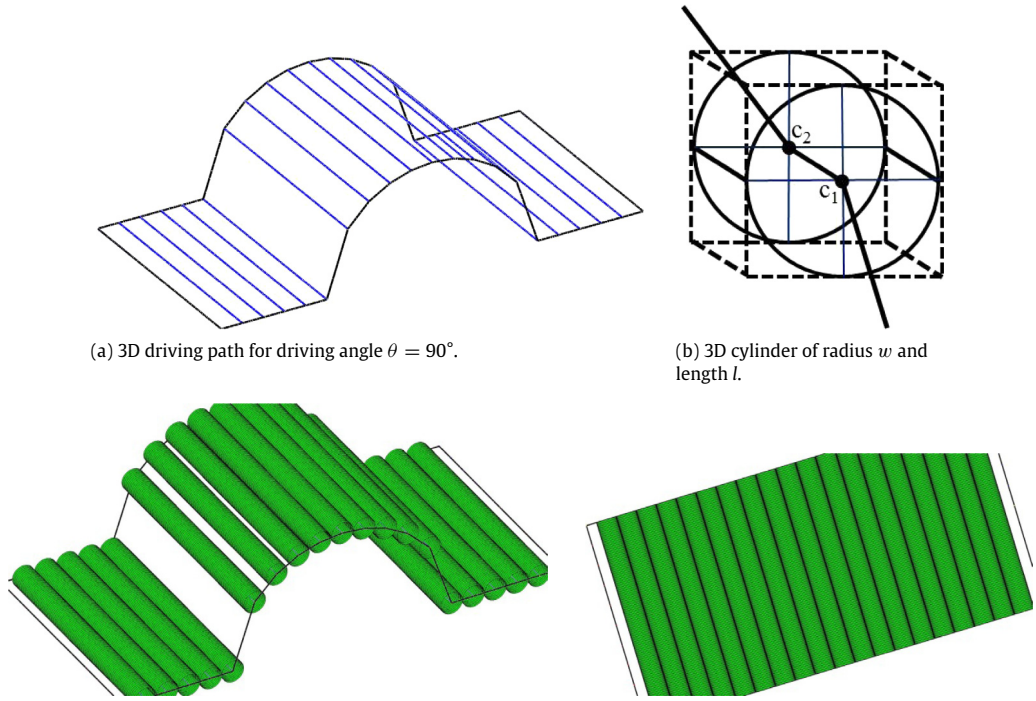

(a) 3D driving path for driving angle $\theta = 90°$.

(b) 3D cylinder of radius w and length l.

(c) Skip areas between swaths in 3D are obvious.

(d) Ignoring elevation suppresses skips.

Fig. 6. Cylindrical approach to assess application efficiency.

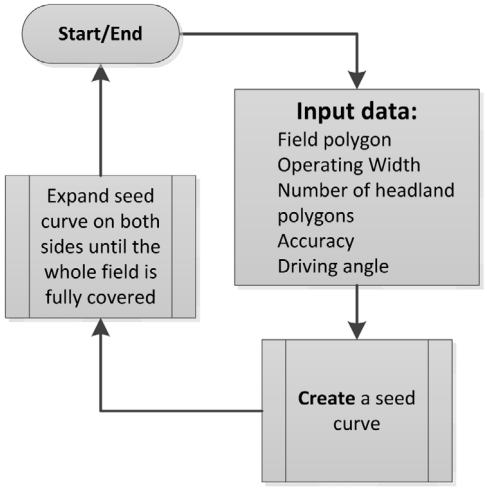

Fig. 7. Flowchart of side-by-side 3D field coverage approach.

intersection between the cylinder and the field surface. The process continues until the entire field is fully covered. A flowchart of the proposed approach is shown in Fig. 7.

3. Results

In this section, the approaches presented in this paper are applied to a hypothetical test with a tailored terrain surface, shown in Fig. 6(a), and then to a real field of an uneven terrain nature to test and validate the developed approaches.

3.1. Hypothetical test field

The field, shown in Fig. 6(a) and again 8(a), is used to demonstrate the functionality of the developed approaches. The field has a flat area of 200 m^2 and a known surface area of 257.08 m^2 and therefore it can be used to validate the approach. The 2D coverage path of the field is generated using the grid approach presented in Section 2.3 for a driving angle of 45°, as it is shown in Fig. 8(b). The 2D coverage path is then projected through the field terrain where bilinear interpolation (BLI) is used to generate smoother 3D coverage path, as it is shown in Fig. 8(c).

The application efficiency of the 3D coverage paths is evaluated for all possible driving angles θ where $0° \leq \theta < 180°$ using the 3D cylindrical approach presented in Section 2.5. The estimated covered area for each driving angle is shown in Fig. 9, from which, it is obvious that full field coverage can be achieved for a driving angle of 0° where field tracks are perpendicular to the sloppy surface of the field so the topography nature does not have any impact on the spaces between swaths, as it is shown in Fig. 10(a). Coverage efficiency dramatically decreases to 84% for a driving angle of 90° where field slope increases the space between swaths, as it is shown in Fig. 10(b). Fig. 6(d) shows the 2D coverage plan for this hypothetical test field for a driving angle of 90°. Although the 2D plan provides full field coverage, the projected 3D plan shows large skipped areas between rows, in the range of 16% of its total surface area that is a significant misuse of the available farmland. Therefore, the need arises for a more efficient and enhanced 3D approach able to provide full coverage regardless of the terrain structure of the field.

In an attempt to eliminate the topographical impact of the field terrain on the spaces between swaths on slopes and in order to achieve full coverage for any driving angle, a side-to-side 3D coverage approach is applied to the above field for a driving angle of 90°. It results in the 3D coverage plan shown in Fig. 11(a) where spaces between adjacent swaths become equal regardless of the terrain nature. The 2D view of the resultant side-to-side 3D coverage plan is shown in Fig. 11(b) where distances between tracks appear to be less in sloppy areas in order to compensate for the terrain impact. By applying the cylindrical approach for estimating coverage efficiency to the side-to-side 3D coverage plan shown in Fig. 11(a) reveal that 100% efficiency can be achieved for any driving angle.

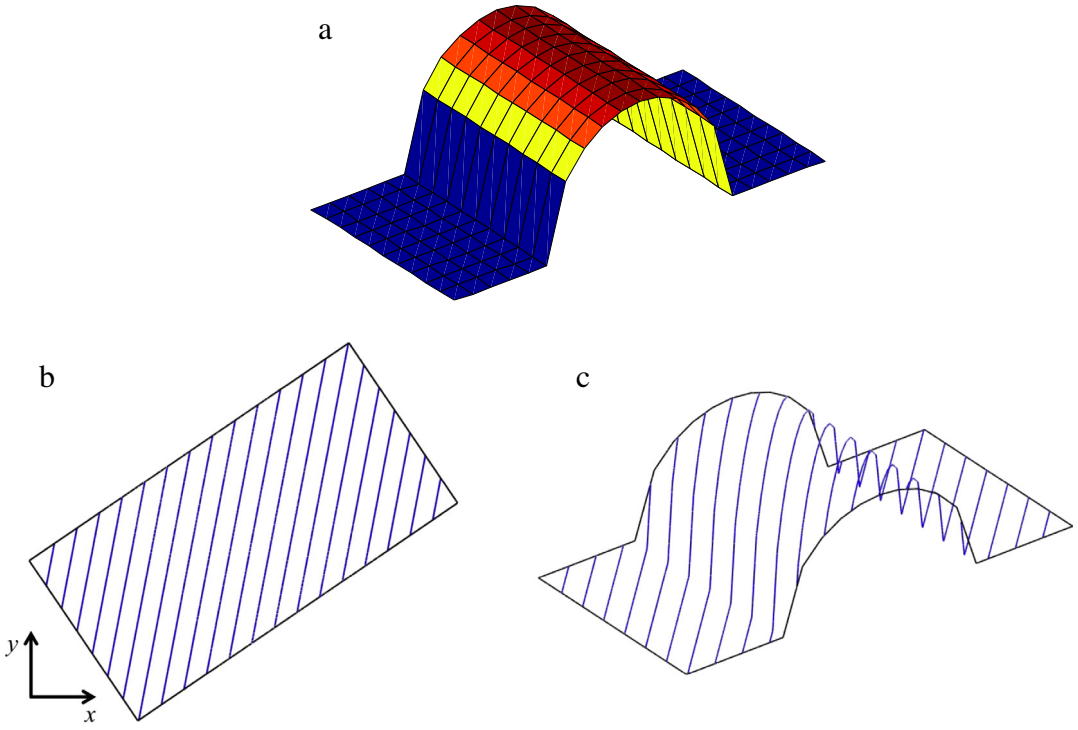

Fig. 8. (a) Artificial field based on a plan with a half cylinder of radius 5 m, and (b) 3D field plan for a driving angle of 45° and 1 m operating width.

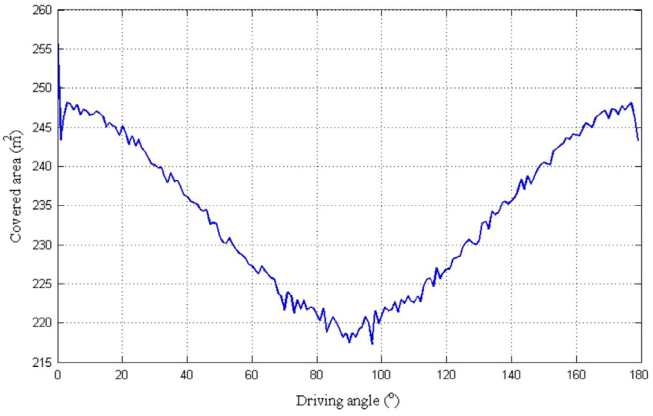

Fig. 9. Covered area (covered area = covering efficiency × surface area) for driving angle $0° \leq \theta < 180°$.

3.2. Experimental test field

A real experimental field, shown in Fig. 12, is used for demonstrating the functionality of the developed approaches. Fig. 12(a) shows the satellite image of the field located at (+56° 30′ 48.10″ N, + 9° 34′ 15.61″ E) which has an area of 21.22 ha. The minimum, maximum, and average elevations on this field are 18.68 m, 42.96 m, and 35.77 m, respectively. The 3D surface view and the contour view of the field's DEM are shown in Fig. 12(b) and (c). Two elevation profiles of the field; from West-to-East and from North-to-South are shown in Fig. 11(d) and (e).

The application efficiency of the 3D coverage plans, obtained using the rapid approach presented in this paper, is evaluated for all possible driving angles θ where $0° \leq \theta < 180°$ using the 3D cylindrical approach presented in Section 2.5, as it is shown in Fig. 13(a). From which it is obvious that the best field coverage (99.53%) was achieved at a driving angle of 90° while lowest field coverage (97.44%) was obtained at a driving angle of 69°. The 3D coverage plan of this field for a driving angle of 90° and 10 m operating width is shown in Fig. 13(b).

To test the capability of the side-to-side 3D coverage algorithm in achieving a full coverage regardless of both the terrain nature and the selected driving angle, the algorithm is applied to the above field for a driving angle of 69° and 10 m operating width. The resultant side-to-side 3D coverage plan is shown in Fig. 14(a) while its 2D view is shown in Fig. 14(b). It might not be very obvious from Fig. 14 that the spaces between

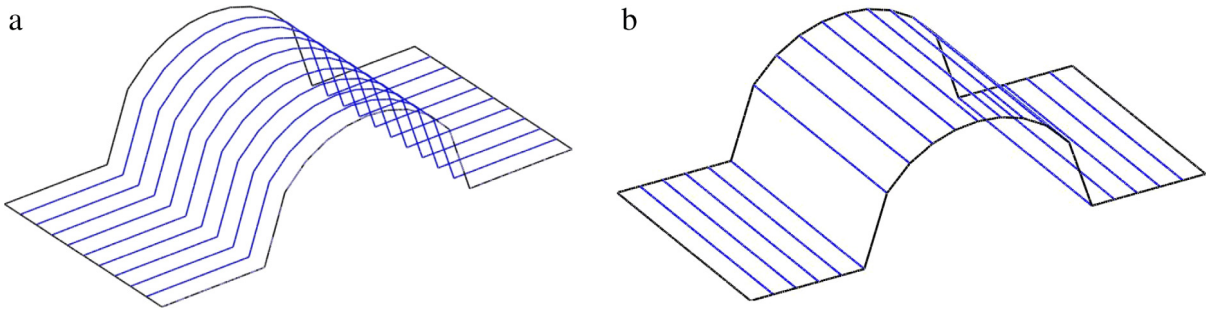

Fig. 10. (a) 3D coverage plan for a driving angle of 0° (100% coverage efficiency), and (b) 3D coverage plan for a driving angle of 90° (84% coverage efficiency).

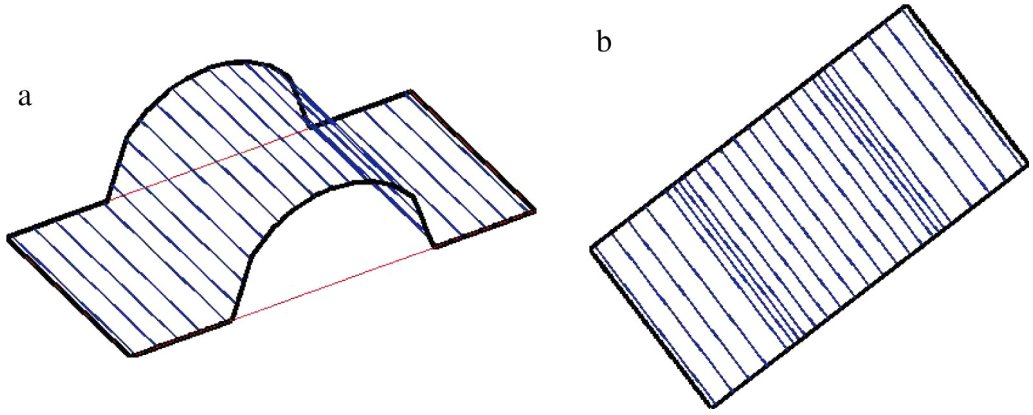

Fig. 11. Side-to-side 3D coverage plan of a field with artificial terrain for an operating width of 1 m and a driving angle of 90°: (a) 3D coverage plan with equal spaces between adjacent swaths, and (b) 2D view of the side-to-side 3D coverage plan.

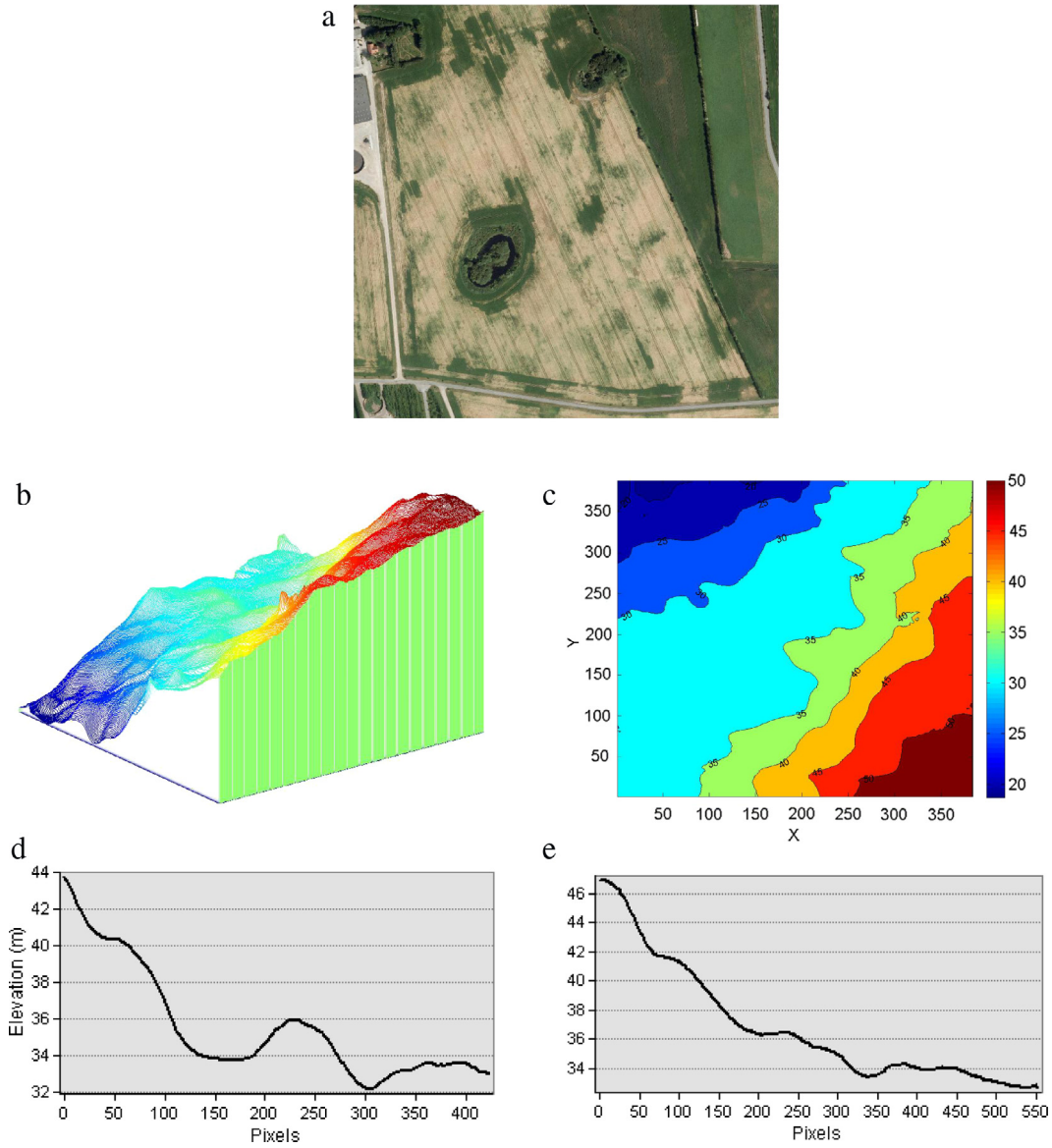

Fig. 12. Experimental field: (a) Satellite image, (b) 3D surface view, (c) contour view based on the DEM information, (d) elevation profile from West-to-East (WE), and (e) elevation profile from North-to-South (NS).

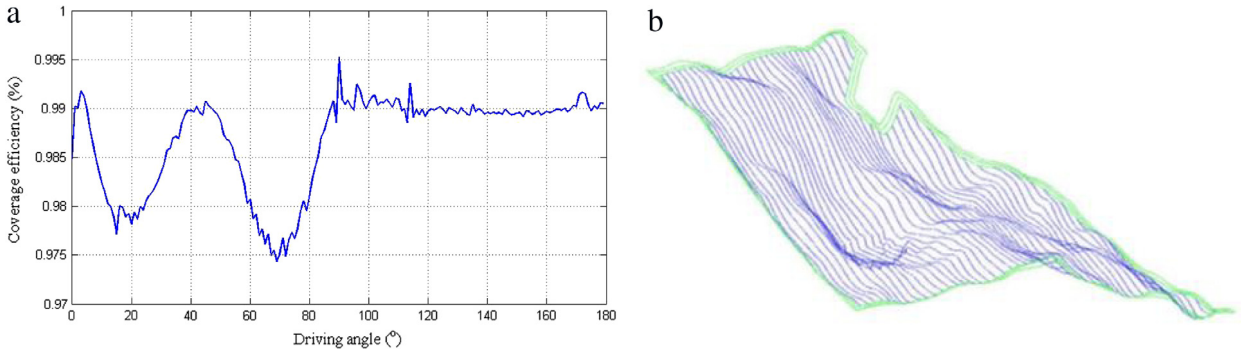

Fig. 13. (a) Coverage efficiency of the 3D coverage plans for driving angle $0^\circ \leq \theta < 180^\circ$, and (b) conventional 3D coverage plan for a driving angle of 90° and 10 m operating width.

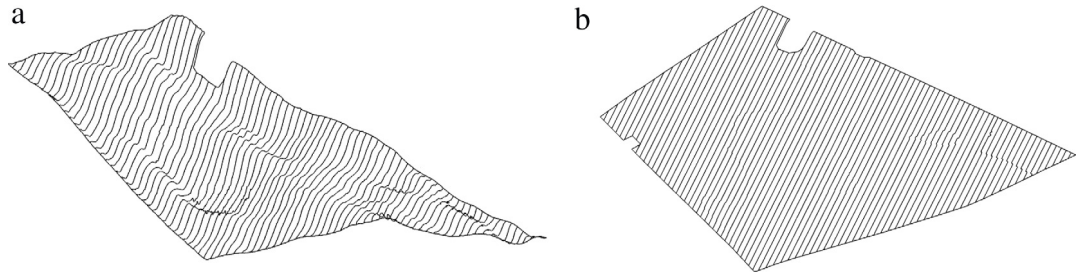

Fig. 14. Side-to-side 3D coverage plan applied to experimental field B for a driving angle of 69° and operating width of 1 m: (a) 3D coverage plan with equal spaces between adjacent swaths, and (b) 2D view of the side-to-side 3D coverage plan.

swaths become equal, however, the cylindrical approach for evaluating coverage efficiency showed that a nearly 100% coverage is achieved. For this field, the cylindrical approach can be used as an evaluation tool to improve area coverage by a value in the range of 2%–3% of the total field area. However, the side-to-side 3D coverage showed superiority in achieving a full coverage regardless of the terrain nature and the driving angle.

4. Conclusions

In this paper, a new 3D coverage algorithm is presented where 2D coverage plans are projected through field terrain. A cylindrical approach for estimating the total skip and/or overlap areas between swaths due to the topographical nature of the field is developed. The proposed approach showed that a significant amount of skip areas could be saved and better used if an appropriate driving angle is chosen. The approach pointed out the fact that an enhanced 3D coverage algorithm capable of eliminating the topographical impact on spaces between swaths is required. A novel side-to-side 3D coverage approach is presented. The developed approach ensures full coverage regardless of the field terrain nature and the chosen driving angle, leaving more freedom for optimization of other factors. The presented approaches for the given test fields showed that savings in the range of 2%–14% of the field surface area can be achieved and better used. Consequently, significant economic benefits can be achieved, especially when these areas are considered over multiple field operations and from year to year. A drawback of the cylindrical approach for estimating coverage efficiency is that it cannot differentiate between skips and overlaps. An analytical approach in which splines are used to smoothly represent field terrain and for generating side-to-side 3D coverage plan is in progress. Interested readers are encouraged to request the Matlab™ code used to implement the approaches presented in this paper from the corresponding author.

Acknowledgments

The authors gratefully acknowledge the constructive comments of anonymous referees.

References

[1] S.M. Pedersen, S. Fountas, H. Have, B.S. Blackmore, Agricultural robots—system analysis and economic feasibility, Precis. Agric. 7 (4) (2006) 295–308.
[2] I.A. Hameed, A. La Cour-Harbo, K.D. Hansen, Task and motion planning for selective weed control using a team of autonomous vehicles, in: Proceedings of 13th IEEE International Conference on Control Automation Robotics & Vision, ICARCV, 10–12 December 2014, Singapore, 2014, pp. 1853–1857. http://dx.doi.org/10.1109/ICARCV.2014.7064598.
[3] M.F. Jensen, M. Nørremark, P. Busato, C.G. Sørensen, D. Bochtis, Coverage planning for capacitated field operations, Part I: Task decomposition, Biosyst. Eng. 139 (2015) 136–148.
[4] T. Oksanen, A. Visala, Coverage path planning algorithms for agricultural field machines, J. Field Robot. 26 (8) (2009) 651–668.
[5] I.A. Hameed, D.D. Bochtis, C.G. Sørensen, M. Nøremark, Automated generation of guidance lines for operational field planning, Biosyst. Eng. 107 (4) (2010) 294–306.
[6] J. Jin, L. Tang, Optimal coverage path planning for arable farming on 2D surfaces, Trans. ASABE 53 (1) (2010) 283–295.
[7] I.A. Hameed, D.D. Bochtis, C.G. Sørensen, Driving angle and track sequence optimization for operational path planning using genetic algorithms, Appl. Eng. Agric. 27 (6) (2011) 1077–1086.
[8] I.A. Hameed, D.D. Bochtis, C.G. Sørensen, An optimized field coverage planning approach for navigation of agricultural robots in fields involving obstacle areas, Int. J. Adv. Rob. Syst. 10 (231) (2013) 1–9.
[9] I.A. Hameed, D.D. Bochtis, C.G. Sørensen, A.L. Jensen, R. Larsen, Optimized driving direction based on a three-dimensional field representation, Comput. Electron. Agric. 91 (2013) 145–153.
[10] M.F. Jensen, D. Bochtis, C.G. Sørensen, Coverage planning for capacitated field operations, part II: Optimisation, Biosyst. Eng. 139 (2015) 149–164.
[11] I.A. Hameed, Intelligent Behavior of Autonomous Vehicles in Outdoor Environment. Technical report ME-TR-2, Aarhus University, Denmark, 2012, ISSN:2245-4594 ISBN: 978-87-92869-38-8.
[12] T.S. Stombaugh, K.B. Koostra, R.C. Dillon, T.G.T. Mueller, C.A. Pike, in: J.V. Stafford (Ed.), Implications of Topography on Field Coverage When Using GPS-Based Guidance, Precision agriculture '07, Wageningen Academic Publisher, University of Kentucky, Wageningen, 2009, pp. 425–432.
[13] B.K. Koostra, T.S. Stombaugh, T.G. Mueller, S.A. Shearer, Evaluaitng the effect of terrain on field area measurements. Paper No. 061045, ASABE, St. Joseph, MI, USA, 2006.
[14] R.C. Dilon, J.-M. Gandonou, B. Koostra, T. Stombaugh, G.T. Mueller, Evaluating the economic impact of field area measurements, in: International Conference on Precision Agriculture Poster and abstract presented at the 8th, Precision Agriculture Center, Minneapolis, MN, USA, 2006.
[15] J. Jin, L. Tang, Coverage path planning on three-dimensional terrain for arable farming, J. Field Robot. 28 (3) (2011) 424–440.
[16] I.A. Hameed, Intelligent coverage path planning for agricultural robots and autonomous machines on three-dimensional terrain, J. Intell. Robot. Syst. 74 (3–4) (2014) 965–983.
[17] R. Buick, A.F. Lange, Assessing efficiency of agricultural chemical application with differential GPS, arcview and spatial analyst, in: Proceedings of Esri International User Conference. Available at: http://proceedings.esri.com/library/userconf/proc98/PROCEED/TO650/PAP622/P622.HTM.

[18] H. Choset, P. Pignon, Coverage path planning: The boustrophedon decomposition, in: Proceedings of the International Conference on Field and Service Robotics.
[19] T.M. Driscoll, Complete coverage path planning in an agricultural environment (Graduate Theses and Dissertations), Iowa State University, USA, 2011.
[20] MathWorks, User's Guide, R2015a, 2015. Retrieved August 16, 2015. From: http://se.mathworks.com/help/matlab/ref/inpolygon.html.
[21] P.J.J. Desmet, Effects of interpolation errors on the analysis of DEMs, Earth Surf. Process. Landf. 22 (6) (1997) 563–580.
[22] S.P. Wechsler, Digital Elevation Model (DEM) uncertainty: evaluation and effect on topographic parameters, in: Proceedings of the 1999 ESRI User Conference, 1999. Available at: http://gis.esri.com/library/userconf/proc99/proceed/papers/pap262/p262.htm.
[23] A.S. Aziz, L.B. Steward, L. Tang, M. Karkee, Utilizing repeated GPS surveys from field operations for development of agricultural field DEMs, Trans. ASABE 52 (4) (2009) 1057–1067.
[24] K.-T. Chang, Introduction to Geographic Information Systems, McGraw-Hill Higher Education, Boston, 2006.

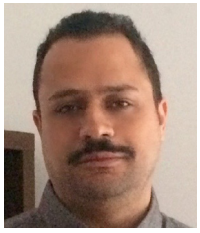

Ibrahim A. Hameed received the B.E. degree in Electronic Engineering and M.Sc. degree in Control Engineering from the Menofia University, Menofia, Egypt, in 1998 and 2005, respectively. He received Ph.D. degree in Industrial Systems and Information Engineering from Korea University, Seoul, South Korea and Ph.D. degree in Mechanical Engineering from Aarhus University, Aarhus, Denmark in 2010 and 2012, respectively. From March 2011 to December 2012, he has been working as an Assistant Professor at Department of Industrial Electronics and Control Engineering, Menofia University, Menofia, Egypt. From January 2013 to July 2015, he has been working as a postdoc at Department of Electronic Systems, Aalborg University, Denmark. Hameed is currently an Associate Professor at Dept. of Automation Engineering, NTNU Ålesund, Aalesund, Norway. His current research interest includes Artificial Intelligence, Control Engineering and Field Robotics.

Anders la Cour-Harbo is an Associate Professor, UAS group manager and Control & Automation Master program coordinator, Aalborg University, Denmark.

Ottar L. Osen received an M.Sc. in Cybernetics from the Norwegian University of Science and Technology (NTNU) in 1991. He is the head of R&D at ICD Software AS and assistant professor in automation engineering at AAUC. He has 14 years of experience from industry and 10 years of experience from academia. His main research interests are artificial intelligence, cybernetics and robotics.